Lawrence Berkeley Laboratory
UNIVERSITY OF CALIFORNIA

Physics Division

Report of the Supersymmetry Subgroup at the Snowmass '86 Summer Study on the Physics of the Superconducting Super Collider, Snowmass, CO, June 23 - July 11, 1986

SIGNALS FOR SUPERSYMMETRY AT THE SSC

R.M. Barnett, D. Atwood, H. Baer, J.A. Grifols, P. Grosse-Wiesmann, J.F. Gunion, H.E. Haber, J. Huston, J. Kalinowski, T. Kamon, G.L. Kane, K. Kondo, A. Mendez, J.P. Mendiburu, S. Mikamo, Y. Morita, D.E. Soper, Y. Takaiwa, X. Tata, F. Ukegawa, R. Wagner, A. Yamashita

November 1986

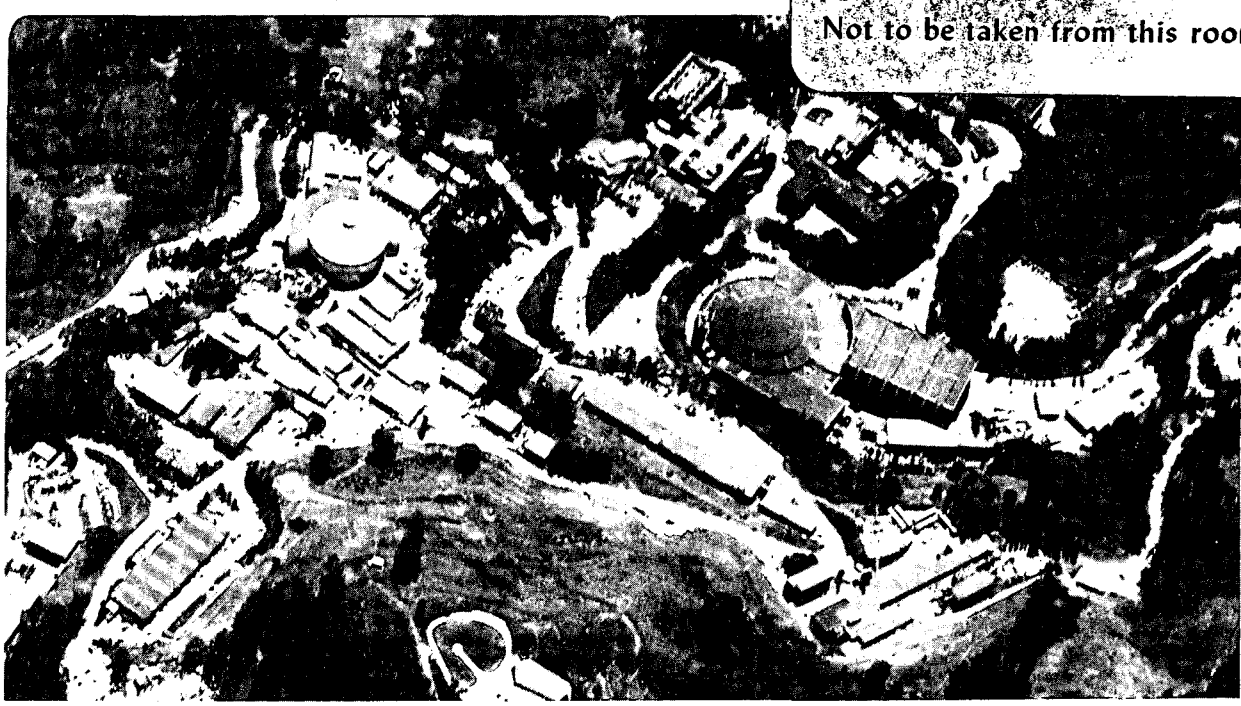

Prepared for the U.S. Department of Energy under Contract DE-AC03-76SF00098

DISCLAIMER

LBL-22497
November 1986

SIGNALS FOR SUPERSYMMETRY AT THE SSC

R. Michael Barnett*
Lawrence Berkeley Laboratory
University of California
Berkeley, California 94720

Group Members and Contributors

D. Atwood (McGill Univ.)
H. Baer (Argonne Natl. Lab.)
J.A. Grifols (Univ. of Barcelona)
P. Grosse-Wiesmann (SLAC)
J.F. Gunion (Univ. of Calif., Davis)
H.E. Haber (Univ. of Calif., Santa Cruz)
J. Huston (Michigan State Univ.)
J. Kalinowski† (Univ. of Calif., Davis)
T. Kamon (Univ. of Tsukuba)
G.L. Kane (Univ. of Michigan)
K. Kondo (Univ. of Tsukuba)
A. Mendez (Univ. of Barcelona)
J.P. Mendiburu (College de France)
S. Mikamo (Fermilab)
Y. Morita (Univ. of Tsukuba)
D.E. Soper (Univ. of Oregon)
Y. Takaiwa (Univ. of Tsukuba)
X. Tata (Univ. of Wisconsin)
F. Ukegawa (Univ. of Tsukuba)
R. Wagner (Argonne Natl. Lab.)
A. Yamashita (Fermilab)

Report of the Supersymmetry Subgroup at the Snowmass '86 Summer Study on the Physics of the Superconducting Super Collider, 23 June – 11 July, 1986, Snowmass, Colorado.

* Supported by the Director, Office of Energy Research, Office of High Energy and Nuclear Physics, Division of High Energy Physics of the U.S. Department of Energy under Contract No. DE-AC03-76SF00098, and by the U.S. National Science Foundation under Agreement No. PHY83-18358.

† On leave of absence from the University of Warsaw

SIGNALS FOR SUPERSYMMETRY AT THE SSC

R. Michael Barnett*
Lawrence Berkeley Laboratory
Berkeley, California 94720

Group Members and Contributors

D. Atwood (McGill Univ.)
H. Baer (Argonne Natl. Lab.)
J.A. Grifols (Univ. of Barcelona)
P. Grosse-Wiesmann (SLAC)
J.F. Gunion (Univ. of Calif., Davis)
H.E. Haber (Univ. of Calif., Santa Cruz)
J. Huston (Michigan State Univ.)
J. Kalinowski† (Univ. of Calif., Davis)
T. Kamon (Univ. of Tsukuba)
G.L. Kane (Univ. of Michigan)
K. Kondo (Univ. of Tsukuba)
A. Mendez (Univ. of Barcelona)
J.P. Mendiburu (College de France)
S. Mikamo (Fermilab)
Y. Morita (Univ. of Tsukuba)
D.E. Soper (Univ. of Oregon)
Y. Takaiwa (Univ. of Tsukuba)
X. Tata (Univ. of Wisconsin)
F. Ukegawa (Univ. of Tsukuba)
R. Wagner (Argonne Natl. Lab.)
A. Yamashita (Fermilab)

Summary

We review progress in setting mass limits for supersymmetric particles. Since missing energy is a prime signal for supersymmetry, we have calculated several sources of "fake" missing energy in ordinary events. The techniques for finding $\tilde{q}\tilde{q}$ and $\tilde{g}\tilde{g}$ production are examined and contrasted for $\sqrt{s} = 0.63$, 2, and 40 TeV; methods of reducing backgrounds are described. The branching ratios of scalar quarks to the lightest supersymmetric particle are calculated with full gaugino mixing. We have considered signals and backgrounds involving hard photons from photino decay and other sources. The process $H \to \widetilde{H}^\circ \tilde{Z}^\circ$ with $\widetilde{H}^\circ \to \gamma\tilde{\gamma}$ and $\tilde{Z}^\circ \to ee\tilde{\gamma}$ was examined in detail and found to have few backgrounds, and to provide a means of detecting a heavy Higgs particle. The direct production of charginos and neutralinos was calculated. Gluinos are considered as constituents of the proton.

I. Introduction

Supersymmetry is a symmetry relating the fermions and bosons.[1] Each boson has a superpartner fermion and vice versa. Empirically we find that no known particle is the superpartner of another known particle. Clearly then supersymmetry is a broken symmetry (otherwise each particle and its superpartner would have the same mass). There are good reasons to believe that the masses of supersymmetric particles will be less than 0.5–1 TeV above those of ordinary particles. However, there is no compelling supersymmetric model to tell us precisely the masses or even the sequence of masses. Our knowledge is, therefore, based on current experimental limits none of which have reached 0.1 TeV.

We are motivated to consider supersymmetry by its scarcity of divergences, by the hope it can provide a mechanism for unifying gravity with other interactions, and by its potential understanding of the gauge hierarchy problem. This latter problem involves the vast difference between the electroweak scale and the scales of grand unification and gravity.

The superpartners expected include the scalar quarks and leptons. There are two spin-zero superpartners for each fermion: $\tilde{f}_L$ denoting the partner of f_L [the SU(2) weak doublet] and $\tilde{f}_R$ the partner of f_R [the SU(2) weak singlet]. For the work reported here, we have usually assumed that $M(\tilde{f}_L) = M(\tilde{f}_R)$ and that 5 or 6 generations of scalar quarks are approximately degenerate in mass.

The gluon, photon, $W^\pm$, Z^0, and neutral and charged Higgs bosons each have a spin 1/2 superpartner. Supersymmetric models require at least two Higgs doublets. The photino, Zino, and neutral Higgsinos mix, and the resulting states are call "neutralinos." The Wino and charged Higgsinos mix and are called "charginos."

The current limits on the masses of scalar quarks and gluinos were provided by the monojet-dijet data of the UA1 experiment for $M(\tilde{\gamma}) \approx 0$.

$$M(\tilde{q}) > 70 \text{ GeV} \tag{1.1}$$

$$M(\tilde{g}) > 60 \text{ GeV} \tag{1.2}$$

Work by Barnett and Haber in this subgroup and by Baer, Karatas, and Tata[2] shows that these limits hold for $M(\tilde{\gamma}) \leq$ 30–40 GeV ($\tilde{q}$) and 20–30 GeV ($\tilde{g}$). The best limit for supersymmetric particles is that for the scalar electron[3] reported this summer by combining the results of three experiments:

$$M(\tilde{e}) > 84 \text{ GeV} \quad \text{for} \quad M(\tilde{\gamma}) \lesssim 3 \text{ GeV}. \tag{1.3}$$

The lower limits for neutralinos and charginos and other superpartners are all less than 25 GeV.

II. Fake Missing Transverse Energy

The predominant signal for supersymmetry at hadron colliders is missing transverse energy, E_T^{miss}. This occurs because the photino (or, more generally, the lightest supersymmetric particle) leaves the detector undetected. However, there are many sources of "fake" missing energy in addition to real sources involving neutrinos. These originate in mismeasurement due to resolution, "holes" in the detector, etc. Our group has considered three sources of mismeasurement; the first two were shown to be small whereas the last is important enough to require attention.

The first source is from transverse energy lost down the beam holes. R. Wagner studied this problem using Monte Carlo generated two-jet events with q_T of the hard scattering set to be greater than 5 GeV/c. In order to have a check on the significance of the results, he studied both events generated by Pythia[4] and Isajet[5]. The samples consisted of 500 events generated by Pythia and 1000 events generated by Isajet.

* Supported by the Director, Office of Energy Research, Office of High Energy and Nuclear Physics, Division of High Energy Physics of the U.S. Department of Energy under Contract No. DE-AC03-76SF00098, and by the U.S. National Science Foundation under Agreement No. PHY83-18358.

† On leave of absence from the University of Warsaw

For each event he calculated the transverse momentum and pseudorapidity of each particle. Particles whose pseudorapidity was greater than a given cut had their vector transverse momentum added to sums of p_{Tx} and p_{Ty}. Because we were dealing with sums for particles with large rapidity, the calculations were performed using double precision variables on a VAX 11/780. Also to further avoid roundoff problems and division by extremely small numbers, particles with $p_T < 1$ keV were ignored. After all particles had been considered, the p_{Tx} and p_{Ty} sums contained the vector missing transverse momentum due to particles that had rapidities larger than the assumed beam hole. The magnitude of this missing p_T vector was then calculated and histogrammed.

The vector transverse momentum sums were in fact calculated for pseudorapidity cuts ranging from 4.0 to 8.0. Figure 1 shows the magnitude of the missing p_T vector versus pseudorapidity cut for both Pythia and Isajet generated events. As is seen the missing transverse momentum due to the beam hole is quite modest, ranging from 1.0 to about 8.5 GeV/c. The standard calorimetry coverage that has been considered for SSC detectors is out to 5.5 in pseudorapidity (this corresponds to being within about 0.5 degrees of the beam line). For this coverage, the average transverse momentum lost through the beam hole is 5.8 GeV/c for Pythia generated events and 4.4 GeV/c for Isajet events. In order to give some idea of the variance of the missing p_T distribution, we show in Figure 2 the missing p_T distribution for a beam hole at pseudorapidity of 5.5. The distribution is quite narrow and, even though the statistics are limited since only 1000 events were generated, beam hole losses do not represent a significant fake missing E_T background. Finally, for completeness Wagner notes that the missing p_T due to the beam hole is increased substantially if one only sums the scalar p_T, i.e. the magnitude of p_T for each particle escaping through the beam hole. For example, for the case of Isajet generated events and a pseudorapidity cutoff at 5.5, he gets an average scalar missing p_T of 31 GeV/c.

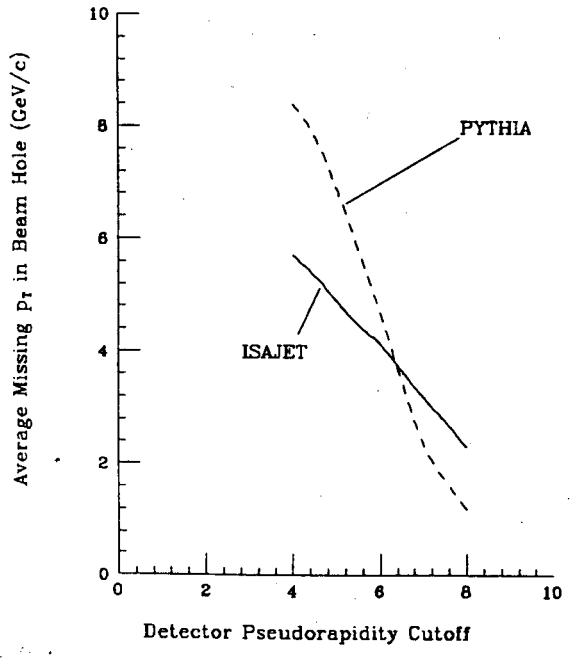

Figure 1. Magnitude of the missing p_T vector due to particle losses in the beam hole versus pseudorapidity cutoff of the detector.

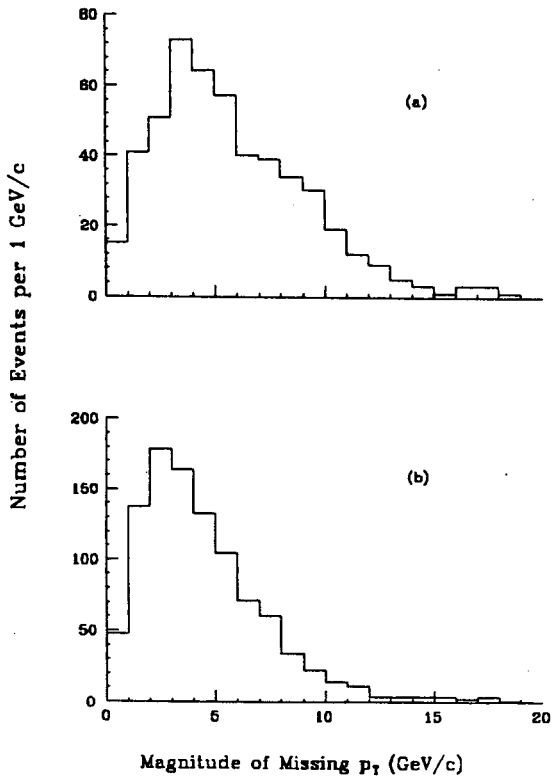

Figure 2. Missing p_T vector magnitude distribution for a detector cutoff of 5.5 in pseudorapidity. (a) 500 Pythia generated events. (b) 1000 Isajet generated events.

The second source of "fake" missing energy we have considered is that due to non-zero calorimetry resolution in minimum-bias events or in the "background" of events with jets. By "background" we mean the remainder of the event when the jets are removed. The resolution of p_T of this background is described[6] by the distribution:

$$e^{-(\delta p_x)^2/2\sigma_x^2} \qquad e^{-(\delta p_y)^2/2\sigma_y^2} \tag{2.1}$$

where for the UA1 experiment[7,8] at the Sp$\bar{\text{p}}$S collider:

$$\sigma_x = \sigma_y = 0.5\sqrt{E_T^{\text{extra}}} \tag{2.2}$$

$$E_T^{\text{extra}} = E_T^{\text{total}} - \sum E_T^{\text{jets}} \tag{2.3}$$

The UA1 collaboration measured the total scalar transverse energy, E_T^{total}, at $\sqrt{s} = 630$ GeV. We assume that E_T^{total} scales as $\sqrt{s}$ although it may well scale more slowly. Figure 3 shows the resultant E_T^{total} distribution at SSC energy. If we now assume that an SSC detector has a resolution similar to that of UA1, we obtain the "fake" missing transverse energy spectrum shown in Fig. 4. This source should not present much of a problem for most supersymmetric signals.

The measurement of jet momenta may provide a more troublesome source of "fake" missing energy, because σ_{jet} in the distribution

$$e^{-(\delta p_{\text{jet}})^2/2\sigma_{\text{jet}}^2} \tag{2.4}$$

is

$$\sigma_{\text{jet}} \approx 0.2 p_{\text{jet}}. \tag{2.5}$$

This resolution leads to much larger "fake" missing energy since p_{jet} can be much larger at SSC. As a result we will have to

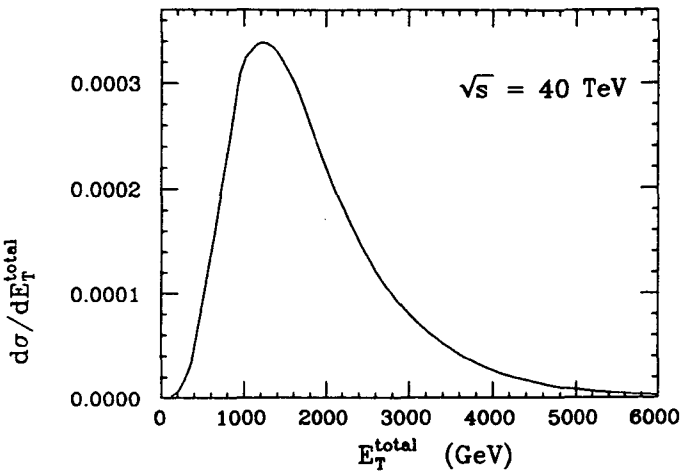

Figure 3. The total scalar transverse energy, $E_T^{\rm total}$, in hard events but excluding hard jets themselves. This was extrapolated from UA1 results to SSC energies by assuming that it scaled with $\sqrt{s}$ [i.e. — $d\sigma/dE_T^{\rm total} = f(E_T^{\rm total}/\sqrt{s})$]. The actual distribution may be softer.

consider cuts to minimize QCD backgrounds to supersymmetric signals. These will be discussed later.

III. Detection of $\tilde{q}\tilde{q}$ and $\tilde{g}\tilde{g}$ Production

Since the supersymmetry report[9] from Snowmass–84, we have learned much more about the observation and detection of gluinos and scalar quarks. This is due to the analysis of UA1 data[10] at the Sp$\bar{\rm p}$S collider. From this we learned about the difficulties of separating signals and backgrounds, but also we learned how to make this separation. UA1 was able to report substantial limits on supersymmetric particles (discussed above).

In making the transition from $\sqrt{s} = 0.63$ TeV to Tevatron energies $\sqrt{s} = 2$ TeV and on to SSC energies $\sqrt{s} = 40$ TeV, some issues become unimportant: 1) fragmentation effects(because the masses are high) and 2) the $E_T^{\rm miss} > 4\sigma$ cut (because we can use much higher $E_T^{\rm miss}$ cuts). For our analyses we have assumed the UA1 resolutions and the UA1 jet definition criterion (see Ref. 6 for a discussion of our modeling of UA1 conditions).

At the SSC we should be able to use the primary cut:

$$E_T^{\rm miss} > 200\text{–}400 \text{ GeV}. \tag{3.1}$$

This will be a powerful cut against most backgrounds. For these events we may also impose a cut (or trigger) on the momentum of the leading jet:

$$E_T(\text{jet}) > 200 \text{ GeV}. \tag{3.2}$$

Figures 5–6 show the cross-sections for missing-energy events before and after $E_T^{\rm miss}$ cuts (and the cuts described below). For design luminosity, these cross sections lead to about 10^6 events per year for lighter gluinos and scalar quarks, and about 10 per year for $M = 4$ TeV taking $B = 1$. (The question of the value of B, the branching ratio to the lightest neutralino, is discussed later.)

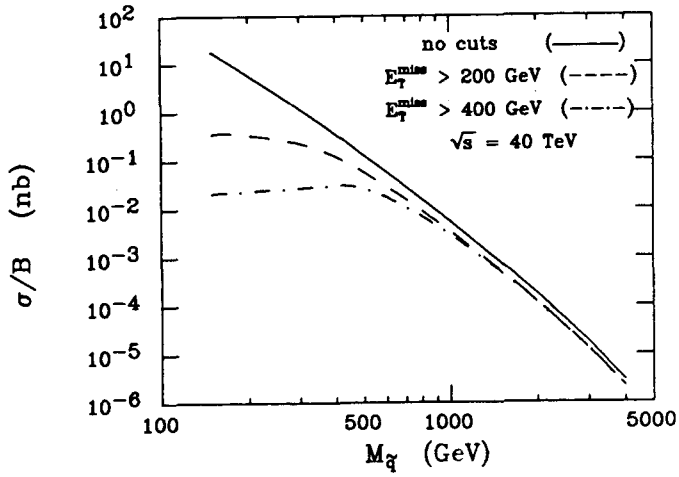

Figure 5. The cross sections divided by B for $\tilde{q}\tilde{q}$ production where $\tilde{q} \to q\tilde{\chi}_1^0$ with $\tilde{\chi}_1^0$ the LSP. B is the branching ratio of $\tilde{q}$ to $q\tilde{\chi}_1^0$. The cuts are as described in the text except that the solid curve is the total cross section before cuts.

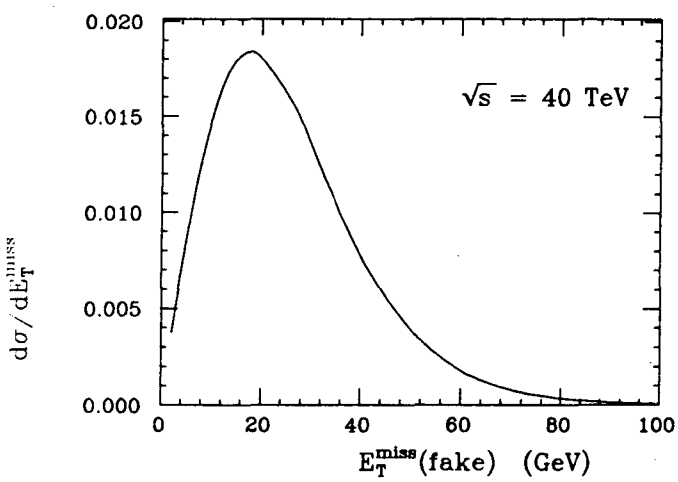

Figure 4. The "fake" missing transverse enegy, $E_T^{\rm miss}$(fake), distribution at $\sqrt{s} = 40$ TeV generated by mismeasurement of $E_T^{\rm total}$ (from Fig. 3). This does not include any fake $E_T^{\rm miss}$ from mismeasurement of hard jets. The resolution is assumed to be the same as that of the UA1 detector

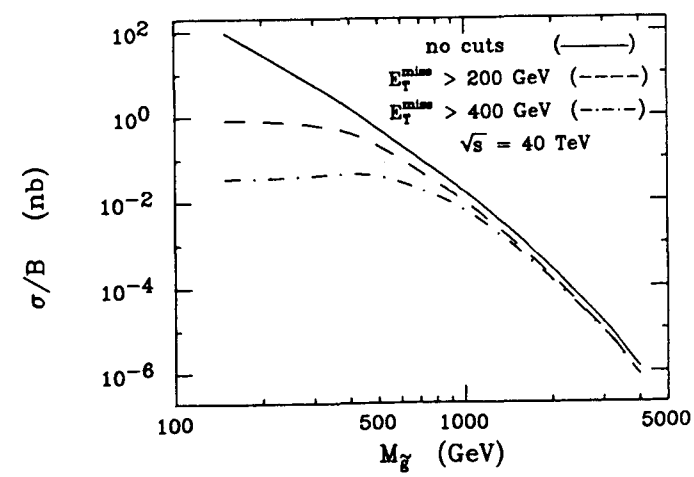

Figure 6. The cross sections divided by B for $\tilde{g}\tilde{g}$ production where $\tilde{q} \to q\bar{q}\tilde{\chi}_1^0$ with $\tilde{\chi}_1^0$ the LSP. B is the branching fraction of $\tilde{g}$ to $q\bar{q}\tilde{\chi}_1^0$. The cuts are described in the text except that the solid curve is the total cross section before cuts.

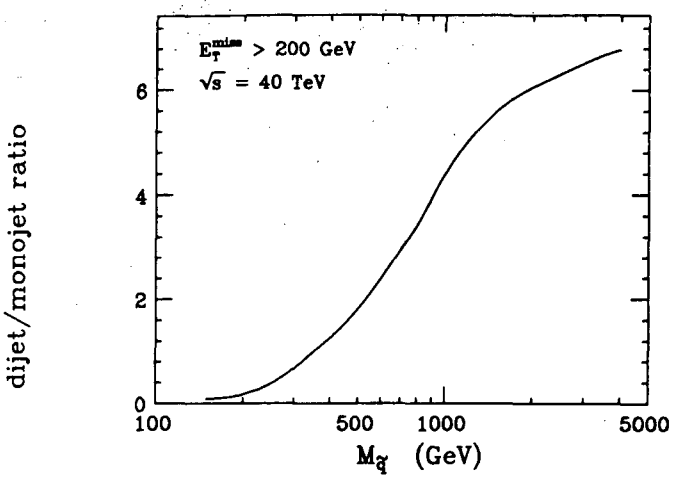

Figure 7. The dijet to monojet ratio in $\tilde{q}\tilde{q}$ production with the cuts described in the text.

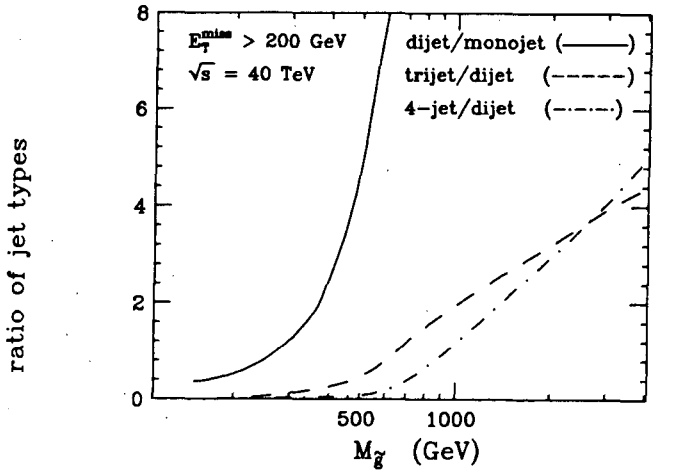

Figure 8. The ratios of events with different numbers of jets originating in $\tilde{g}\tilde{g}$ production. The cuts used are described in the text.

Next we may ask about the topology of the events. This depends on our definition of jets. UA1 required $E_T^{\rm jet} > 12$ GeV for a jet to be called a jet (otherwise the energy was thrown in with the "background" scalar transverse energy). For SSC energies we have chosen a very high cut $E_T^{\rm jet} > 100$ GeV. Fig. 7 shows that $\tilde{q}\tilde{q}$ production is dominated by dijets for $M_{\tilde{q}} > 350$ GeV even with our $E_T^{\rm miss} > 200$ GeV cut. In Fig. 8 we see that dijets dominate in $\tilde{g}\tilde{g}$ production from $M_{\tilde{g}} = 250$ to 650 GeV, but for higher masses, trijets and quadrajets dominate. The search for gluinos and scalar quarks, therefore, requires the consideration of all missing energy events; the topology will give us important clues as to the masses and identity of the observed particles.

The UA1 collaboration was able to identify powerful cuts for reducing the QCD backgrounds of two jet events. When one of the jets is mismeasured, one can obtain large missing energy and the appearance of one-jet topology. To make these cuts UA1 lowered the definition of a jet from $E_T^{\rm jet} = 12$ to 8 GeV. They then required

$$\text{angle}(\vec{p}_{\text{jet}(2)}, -\vec{p}_{\text{jet}(1)}) > 30^\circ \tag{3.3}$$

$$\text{angle}(\vec{p}_{\text{jet}(2)}, \vec{p}_T^{\,\rm miss}) > 30^\circ \tag{3.4}$$

Although these cuts also eliminated $\tilde{g}\tilde{g}$ events for very small $M_{\tilde{g}}$, they should have little impact for the masses of interest at SSC (although continuing to eliminate QCD backgrounds). For the purpose of these cuts at SSC energies, we chose to lower the $E_T^{\rm jet} > 100$ GeV jet definition to $E_T^{\rm jet} > 60$ GeV. One can require the angles to be greater than 45° without losing many monojet or dijet events of supersymmetric origin.

These cuts, however, only apply to monojet and dijet events. For the more general topologies expected at $\sqrt{s} = 2$–40 TeV, new strategies must be devised. These have been examined by Atwood, by Barnett and Haber, and by Kamon and Kondo.

Atwood considered QCD events and began by assuming (as do previous authors) that jet mismeasurement is parallel to the jet momentum. Then (as above) the error in measuring the i'th parton's momentum, $\vec{p}_i$, is

$$\sigma_i = \ell|\vec{p}_i| \qquad \ell \approx 0.2 \tag{3.5}$$

The measured momentum is

$$\vec{p}_i^{\,\rm meas} = \vec{p}_i + \lambda_i \hat{p}_i \qquad \hat{p}_i \equiv \vec{p}_i/|\vec{p}_i| \tag{3.6}$$

with probability

$$\frac{1}{\sqrt{2\pi}\sigma_i} \exp\left(-\frac{\lambda_i^2}{2\sigma_i^2}\right) d\lambda_i \tag{3.7}$$

The above formulae hold for transverse momenta also if we add the subscript T to $\vec{p}_i$, $\vec{p}_i^{\,\rm meas}$, and σ_i (because $\sigma_i \propto p_i$).

If we define

$$p_{Ti} \equiv \begin{bmatrix} p_{xi} \\ p_{yi} \end{bmatrix}, \tag{3.8}$$

then the missing transverse momentum in QCD events is

$$p_T^{\rm miss} = -\sum_i p_i^{\rm meas} = -\sum_i \lambda_i \hat{p}_{Ti}. \tag{3.9}$$

The probability of a given $p_T^{\rm miss}$ is

$$\frac{1}{2\pi\sqrt{\det(E)}} \exp\left(-\frac{1}{2} p_T^{\rm miss} E^{-1} p_T^{\rm miss}\right) \tag{3.10}$$

where the error matrix, E, is

$$E = \sum \sigma_{Ti}^2 \hat{p}_{Ti} \hat{p}_{Ti}^{\mathcal{T}} = \sum \ell^2 p_{Ti} p_{Ti}^{\mathcal{T}} \tag{3.11}$$

(superscript $\mathcal{T}$ means transposed). For QCD trijet events, one can deduce from momentum conservation the relation:

$$|p_{T1}| : |p_{T2}| : |p_{T3}| = \sin\theta_1 : \sin\theta_2 : \sin\theta_3. \tag{3.12}$$

where θ_i is the angle between p_{Tj} and p_{Tk}. The error matrix can then be written as

$$\begin{aligned} E &= \left(\frac{E_T}{\sum \sin\theta_i}\right)^2 \sum \ell^2 \sin^2\theta_i \hat{p}_{Ti} \hat{p}_{Ti}^{\mathcal{T}} \\ &= \left(\frac{E_T}{\sum \sin\theta_i}\right)^2 \sum \ell^2 \sin^2\theta_i \hat{p}_{Ti}^{\rm meas} \hat{p}_{Ti}^{\rm meas\,\mathcal{T}} \end{aligned} \tag{3.13}$$

where $E_T \equiv p_{T1} + p_{T2} + p_{T3}$. Therefore, from the measured event one can deduce the ratios between the components of E, and hence the shape of the probability contours in $p_T^{\rm miss}$.

Rotating to a frame where E is diagonal, we find

$$E = \begin{bmatrix} \sigma_x^2 & 0 \\ 0 & \sigma_y^2 \end{bmatrix} \tag{3.14}$$

and thus

$$\text{Prob}(p_T^{\text{miss}}) = \frac{1}{2\pi\sqrt{\det(E)}} p_T^{\text{miss}} \times \int_0^{2\pi} \exp\left[-(p_T^{\text{miss}})^2\left(\frac{\cos^2\theta}{2\sigma_x^2} + \frac{\sin^2\theta}{2\sigma_y^2}\right)\right] d\theta \tag{3.15}$$

For $\sigma_x = \sigma_y$

$$\text{Prob}(p_T^{\text{miss}}) = \frac{1}{\sigma_x^2} p_T^{\text{miss}} \quad \exp\left[-\frac{(p_T^{\text{miss}})^2}{2\sigma_x^2}\right]. \tag{3.16}$$

For $\sigma_x \neq \sigma_y$ one can show

$$\text{Prob}(p_T^{\text{miss}}) \approx \frac{4}{\sqrt{2\pi|\sigma_x^2 - \sigma_y^2|}} \exp\left[-\frac{(p_T^{\text{miss}})^2}{2\text{Max}(\sigma_x^2, \sigma_y^2)}\right]. \tag{3.17}$$

valid if $p_T^{\text{miss}} > \sigma_x, \sigma_y$.

Notice that the major axis of the error ellipse gives the dominant contribution to the p_T^{miss} distribution for large p_T^{miss}. Since in the three-jet case we can tell, from the measured jets, the shape of the error ellipse, we know which direction this is. One cut to eliminate QCD trijet events is readily apparent: eliminate events in which

$$\text{angle}(\vec{p}_T^{\text{miss}}, \text{major axis of } E) < \theta_0, \tag{3.18}$$

where we assume the event results from mismeasurement.

Alternatively, we can try to make the best guess for the parton momenta of the original event (before mismeasurement). As shown in Eq. 3.12, for a given QCD event, we know the ratios of the true p_{T_i} and not their absolute magnitude. The probability of measuring p_i^{meas} is

$$\frac{1}{(2\pi)^{\frac{3}{2}}\ell^3 p_1^* p_2^* p_3^*} \exp\left[-\sum \frac{|p_i^*| - |p_i^{\text{meas}}|)^2}{2(\ell p_i^*)^2}\right] \tag{3.19}$$

where we add a superscript "*" to the choice of p_i which maximizes this probability. Substituting p_i^* in Eq. 3.11 for E (which we then call E^*) and using Eq. 3.10, another possible cut for eliminating QCD trijet events is to reject events with

$$\frac{1}{2} p_T^{\text{miss}\,T} E^{*-1} p_T^{\text{miss}} < -\ell n\, P_0 \tag{3.20}$$

for some probability, P_0. This has the effect of cutting E_T^{miss} from an elliptical portion of the plane similar to the error ellipse.

Kamon and Kondo have developed a likelihood method for separating $\tilde{g}\tilde{g}$ production from background. We will discuss it briefly here, since the details are given in their contribution to these proceedings. They were motivated to find which kinematical variables were the most useful and to find a general method for finding such variables. Their method consists of the following steps:

1). Choose the initial kinematical parameters x_i For their example, they chose E_T^{miss}, p_E, p_{out}, E_T(total), the number of clusters with $E_T > 10$ GeV, and six other variables.

2). Generate the signal events and calculate the distribution in each variable and find the mean value $\langle x_i \rangle$.

3). Calculate the covariance matrix C_{ij} of variables around its mean value:

$$C_{ij} = \sum \frac{(x_i - \langle x_i \rangle)(x_j - \langle x_j \rangle)}{N\sigma_i\sigma_j} \tag{3.21}$$

where N is the total number of events.

4). Diagonalize C_{ij} and find the transformation matrix U_{ij}, the eigenvalues E_{ii}, and the new set of variables (eigenvectors) z_i where

$$z_i = \sum U_{ij}^{-1}(y_j - \langle y_j \rangle)/\sqrt{E_{ij}} \tag{3.22}$$

for

$$y_j \equiv (x_j - \langle x_j \rangle)/\sigma_j \tag{3.23}$$

5). Obtain the signal probability functions $P_{si}(z_i)$ and by generating background events, the background probability functions $P_{bi}(z_i)$.

6). Find the effectiveness of a variable z_i in separating signal and background with the separation parameter S_i

$$S_i = \frac{1}{2}\int |P_{si}(z) - P_{bi}(z)| dz. \tag{3.24}$$

S_i indicates perfect separation while $S_i = 0$ indicates that z_i has no value in separating signal and background. Keep an appropriate number m of the variables with large S_i.

7.) Generate new sets of signal and background events.

8.) For these new events, calculate for each event the ratio of the signal probability to the background probability

$$r = \frac{P_{s1}(z_1)P_{s2}(z_2)\ldots P_{sm}(z_m)}{P_{b1}(z_1)P_{b2}(z_2)\ldots P_{bm}(z_m)} \tag{3.25}$$

9.) Define the likelihood that the event is signal rather than background by

$$L = \ell n\, r \tag{3.26}$$

If the likelihood distribution of events is well separated between signal and background, then this method of event identification works.

It should be noted that only linear combinations of the initial variables can be generated (not products, quotients, logarithms, etc.). Therefore the effectiveness of the method strongly depends on the choice of initial parameters.

For the example variables chosen by Kamon and Kondo (with $M_{\tilde{g}} = 200$ GeV), they could obtain a rejection power against background of 1900 with signal acceptance of 6.6%. This gave a signal-to-background ratio of 6.2.

Barnett and Haber examined a variety of variables in order to separate trijet and quadrajet events in $\tilde{g}\tilde{g}$ production from those in QCD ($ggg, gq\bar{q}$, etc.). Here we discuss five of these variables. The results reported here for QCD are with matrix element $M = 1$ and therefore are normalized arbitrarily. Results with the full matrix element are in preparation and will be reported elsewhere.

Since the most immediate results will come from the Tevatron, we have chosen to show distributions at $\sqrt{s} = 1.7$ TeV and $M_{\tilde{g}} = 100$ GeV ($M_{\tilde{q}} = 2M_{\tilde{g}}$). Here we chose the cuts $E_T^{\text{miss}} > 40$ GeV, $E_T^{\text{jet}(1)} > 40$ GeV, and jet definition $E_T^{\text{jet}} > 20$ GeV.

Not surprisingly, the E_T^{miss} distribution, Fig. 9, is more sharply peaked for QCD trijets than for those from $\tilde{g}\tilde{g}$ production. This means increasing the E_T^{miss} cut will increase the signal-to-background ratio. In Fig. 10 we consider the transverse energy of the leading jet, $E_T^{\text{jet}(1)}$. In order to obtain significant fake missing energy ($E_T^{\text{miss}} > 40$ GeV), we expect we will need very energetic jets since the mismeasurement is proportional to jet energy. This is precisely what we see in Fig. 10; the jets in background (QCD) events are much more energetic than those from supersymmetric origin. The latter are, of course, dependent on $M_{\tilde{g}}$. A useful cut may be to place

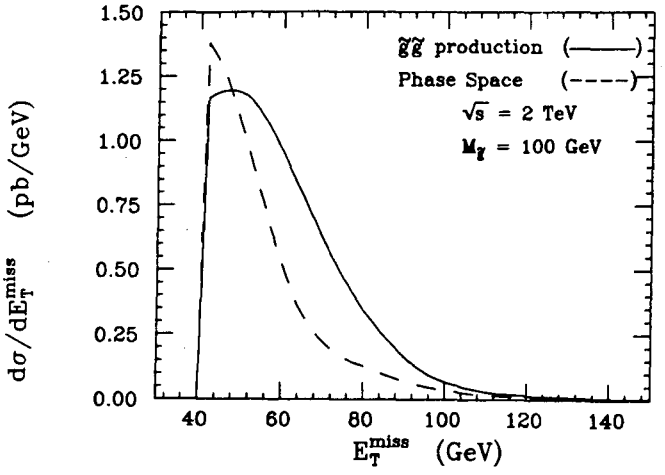

Figure 9. The $E_T^{\rm miss}$ distribution for trijets events at Tevatron energies. Events were required to have $E_T^{\rm miss} > 40$ GeV, $E_T^{\rm jet(1)} > 40$ GeV, and $E_T^{\rm jet(2,3)} > 20$ GeV; the UA1 detector resolution was assumed. The solid curve is for $\tilde{g}\tilde{g}$ production and assumes $\tilde{g} \to q\bar{q}\tilde{\gamma}$. The dashed curve has the phase space for QCD trijets but has a constant matrix element (so normalization is not significant).

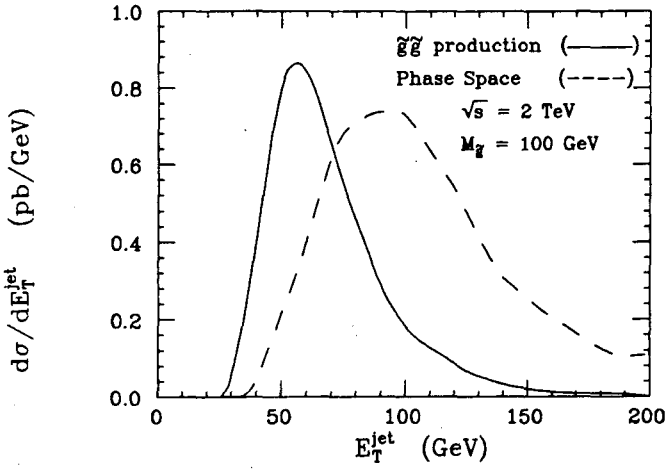

Figure 10. The $E_T^{\rm jet}$ distribution for leading jets in trijet events at Tevatron energies. Other details are described in Fig. 9.

an upper limit on $E_T^{\rm jet(1)}$ (e.g. — $E_T^{\rm jet(1)} < 80$–100 GeV at Tevatron energies); this would be in addition to the lower limit.

Two additional variables we found useful were

$$\phi_{1m} \equiv \text{angle}(\vec{p}_T^{\,\rm jet(1)}, \vec{p}_T^{\,\rm miss}) \tag{3.27}$$

$$\phi_{2m} \equiv \text{angle}(\vec{p}_T^{\,\rm jet(2)}, \vec{p}_T^{\,\rm miss}) \tag{3.28}$$

Examination of Figs. 11 and 12 shows that the distributions for ϕ_{1m} and ϕ_{2m} are dramatically different for QCD trijets and for supersymmetric trijets. Clearly cuts such as $\phi_{2m} > 30°$ and $\phi_{1m} > 160°$ would greatly reduce the background.

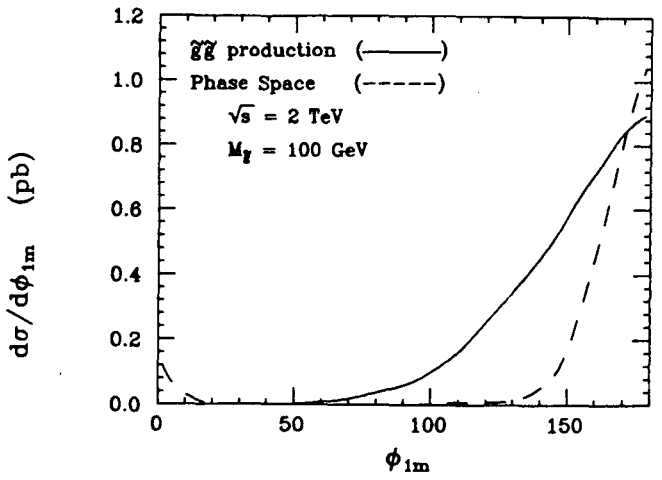

Figure 11. The ϕ_{1m} distribution (described in text) for trijet events at Tevatron energies. Other details are described in Fig. 9.

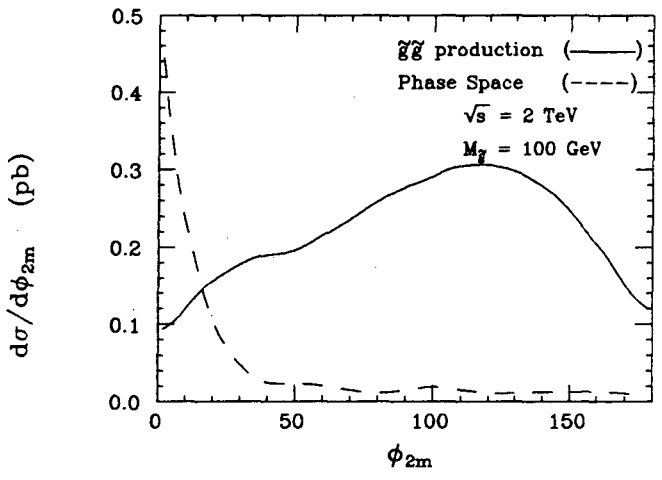

Figure 12. The ϕ_{2m} trijet events at Tevatron energies. Other details are described in Fig. 9.

A final variable we found interesting was β, the longitudinal velocity by which we boost a given trijet event in order to make it become coplanar. Since $\tilde{g}\tilde{g}$ production has two unobserved photinos, we speculated that the β distributions for signal and background would be quite different. We begin by writing the appropriate boost for a 4-vector p as

$$\begin{pmatrix} p_0 \\ p_T \\ p_z \end{pmatrix} \to \begin{pmatrix} p_0 \cosh\eta + p_z \sinh\eta \\ p_T \\ p_0 \sinh\eta + p_z \cosh\eta \end{pmatrix} \tag{3.29}$$

where

$$\begin{aligned} \gamma &= \cosh\eta \qquad \beta\gamma = \sinh\eta \\ \beta &= \tanh\eta \qquad \gamma = (1-\beta^2)^{-\frac{1}{2}} \end{aligned} \tag{3.30}$$

Let us now consider the matrix P of the three jet momenta, a, b, and c in the boosted frame:

$$P = \begin{pmatrix} a_1 & a_2 & a_0\sinh\eta + a_3\cosh\eta \\ b_1 & b_2 & b_0\sinh\eta + b_3\cosh\eta \\ c_1 & b_2 & c_0\sinh\eta + c_3\cosh\eta \end{pmatrix} \tag{3.31}$$

To solve for β we set $\det(P) = 0$. This gives

$$Y \sinh\eta + X \cosh\eta = 0 \tag{3.32}$$

$$X = a_1b_2c_3 - a_1b_3c_2 - a_2b_1c_3 + a_2b_3c_1 + a_3b_1c_2 - a_3b_2c_1 \tag{3.33}$$

$$Y = X(3 \longleftrightarrow 0) \tag{3.34}$$

We now note that

$$X = (\vec{a} \times \vec{b}) \cdot \vec{c} \qquad Y = (\vec{a}\,' \times \vec{b}\,') \cdot \vec{c}\,' \tag{3.35}$$

where we define the primed momenta as

$$\vec{p}\,' = (p_1, p_2, p_0) \tag{3.36}$$

so that

$$\beta = \tanh\eta = \left[-\frac{(\vec{a} \times \vec{b}) \cdot \vec{c}}{(\vec{a}\,' \times \vec{b}\,') \cdot \vec{c}\,'} \right] \tag{3.37}$$

Having derived β, the velocity of the frame in which a given event is coplanar, we can now look at the distribution in β for QCD and supersymmetric trijets, Fig. 13. This variable does not have as much impact as other variables discussed above.

One may see evidence for some of the findings described above by looking at simulated events. In Figs. 14 and 15 we show simulated QCD and supersymmetric events.

A primary difference between results for $\tilde{q}\tilde{q}$ and $\tilde{g}\tilde{g}$ production at the Sp$\bar{\text{p}}$S collider and results at the Tevatron and SSC is that the dominant direct decay of gluinos and scalar quarks will not necessarily be to photinos. The allowed decay modes are likely to include other neutralinos and charginos. To our good fortune the cross sections (Figs. 5 and 6) for gluino and scalar quark production are very high at SSC energies, so that a loss of a factor of 10 due to branching fractions is not important. However, this may be a problem at Tevatron energies, depending on the details of a given scenario.

Baer and Berger[11] have examined this question at Tevatron energies in the context of a plausible scenario. They chose

$$M_{\widetilde{W}} = 60 \text{ GeV} \qquad M_{\widetilde{Z}} = 68 \text{ GeV} \qquad M_{\tilde{\gamma}} = 8 \text{ GeV} \tag{3.38}$$

and found the results displayed in Fig. 16. As shown, the branching fractions of $\tilde{u}_R$ and $\tilde{d}_R$ to photinos remain very high, but $\tilde{u}_L$ and $\tilde{d}_L$ drop to 25% and 5% respectively. Baer and

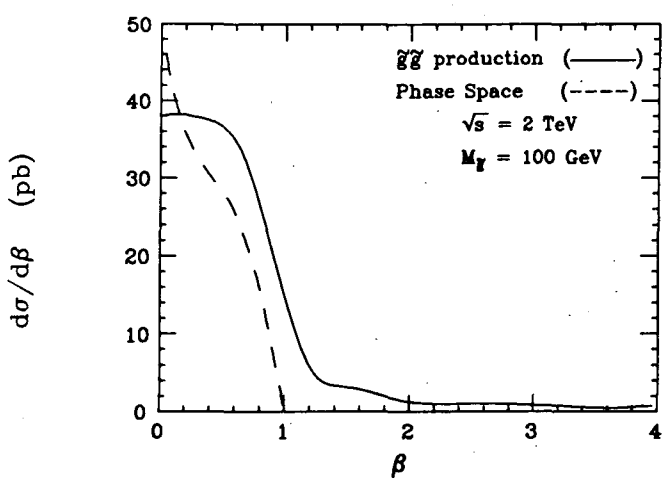

Figure 13. The β distribution (described in text) for trijet events at Tevatron energies. Other details are described in Fig. 9.

Tata have extended their calculation for gluino branching fractions to higher masses and found that the photino mode drops asymptotically to about 20% (for $M_{\tilde{g}} \gtrsim 400$ GeV); for this calculation they chose $M_{\widetilde{W}} = M_W$ and $M_{\widetilde{Z}} = M_Z$.

Barnett and Haber[12] examined the branching fractions of scalar quarks for masses of interest at SSC and for a very wide range of scenarios. They have allowed full mixing in the neutralino and chargino sectors. Since with this generality one never finds pure photino states, the question of interest is the branching fraction to the lightest supersymmetric particle (LSP) assumed to be some neutralino (labeled $\tilde{\chi}_1^0$). If the LSP is a pure Higgsino, then the branching fraction is quite small (or zero) depending on whether we are considering $\tilde{u}$, $\tilde{d}$, $\tilde{s}$, $\tilde{c}$, $\tilde{b}$, or $\tilde{t}$.

Neutralino mixing can be described in terms of several parameters:

a) $\tan\beta = v_2/v_1$ where v_2 and v_1 are the vacuum expectation values of the H_2 and H_1.
b) μ — a supersymmetric Higgs mass term.
c) M, M' — gaugino Majorana mass terms corresponding to masses for the weak interaction eigenstates $\widetilde{W}_3$ and $\widetilde{B}$ respectively (from which $\tilde{\gamma}$ and $\tilde{Z}^0$ can be defined).

In many models (those with a common mass for the SU(3), SU(2), and U(1) gauginos at the grand unification scale) M and M' are related by

$$\frac{M'}{M} = \frac{5}{3}\frac{g'^2}{g^2} = \frac{5}{3}\tan^2\theta_W. \tag{3.39}$$

In terms of the weak interaction eigenstate basis $(\widetilde{B}, \widetilde{W}_3, \widetilde{H}_1, \widetilde{H}_2)$, the mass matrix is

$$\begin{pmatrix} M' & 0 & -m_Z s_W c_\beta & m_Z s_W s_\beta \\ 0 & M & m_Z c_W c_\beta & -m_Z c_W s_\beta \\ -m_Z s_W c_\beta & m_Z c_W c_\beta & 0 & -\mu \\ m_Z s_W s_\beta & -m_Z c_W s_\beta & -\mu & 0 \end{pmatrix} \tag{3.40}$$

where $s_W \equiv \sin\theta_W$, $c_W \equiv \cos\theta_W$, $s_\beta \equiv \sin\beta$, $c_\beta \equiv \cos\beta$.

The branching fractions for $\tilde{q}_L$ and $\tilde{q}_R$ are in general very different. The $\tilde{q}_L$ prefer to decay to charginos whereas $\tilde{q}_R$ cannot decay to charginos. In fact as μ becomes comparable to other mass parameters, the branching fractions of $\tilde{q}_L$ and $\tilde{q}_R$ to the LSP ($\tilde{\chi}_1^0$) approach 0 and 1 respectively.

The next issue is which $\tilde{q}$ are produced. $\tilde{q}\tilde{q}$ pair production is the primary signal when $M_{\tilde{q}} < M_{\tilde{g}}$ (as suggested by some superstring models). This may be $\tilde{q}_L\tilde{q}_L$, $\tilde{q}_R\tilde{q}_R$, $\tilde{q}_L\tilde{q}_R$, or $\tilde{q}_R\tilde{q}_L$. We have not at this time calculated which mode is most commonly produced, but our expectations are that at SSC energies gluon-gluon scattering dominates, and the first two modes will therefore be predominant. (The same argument applies to $\tilde{u}_L\tilde{d}_L$ and $\tilde{u}_R\tilde{d}_R$.) Given that $B(\tilde{q}_L \to q\tilde{\chi}_1^0)$ is small, it would be fortunate if $\tilde{q}_R\tilde{q}_R$ occurs with a substantial fraction, since it would preserve our best signal (two jets and very large E_T^{miss}).

When scalar quarks do not decay to the LSP ($\tilde{\chi}_1^0$), then our primary signal is suppressed. In order to study this suppression, for "all" scenarios, we first assume that $\tilde{q}_L\tilde{q}_R$ is not important so that we may plot the square of the branching ratios of the two scalar quarks produced. We then take an average over $\tilde{q}_L\tilde{q}_L$ and $\tilde{q}_R\tilde{q}_R$ and over up and down flavors. To the extent that $\tilde{q}_L\tilde{q}_R$ can contribute, our numbers might be reduced somewhat.

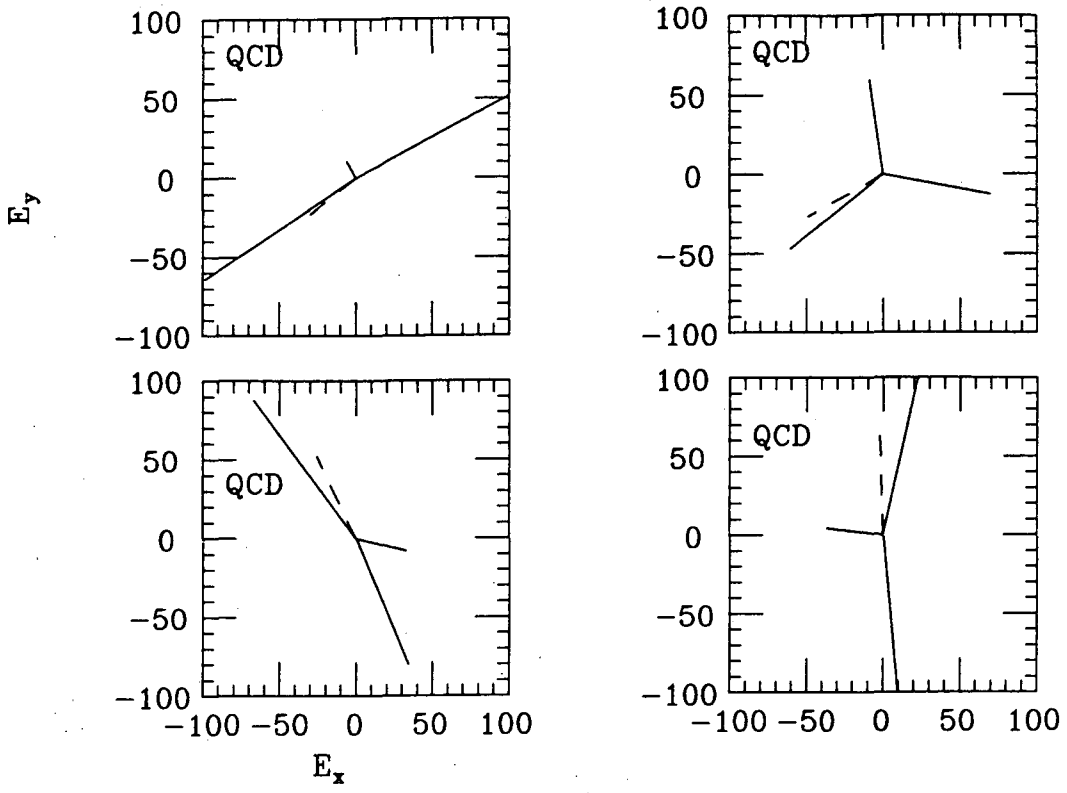

Figure 14. Simulated trijet events with large $E_T^{\rm miss}$ (shown with dashed line) from QCD. The beam is perpendicular to the figure. The x and y axes are the energy of the jets in the x and y directions.

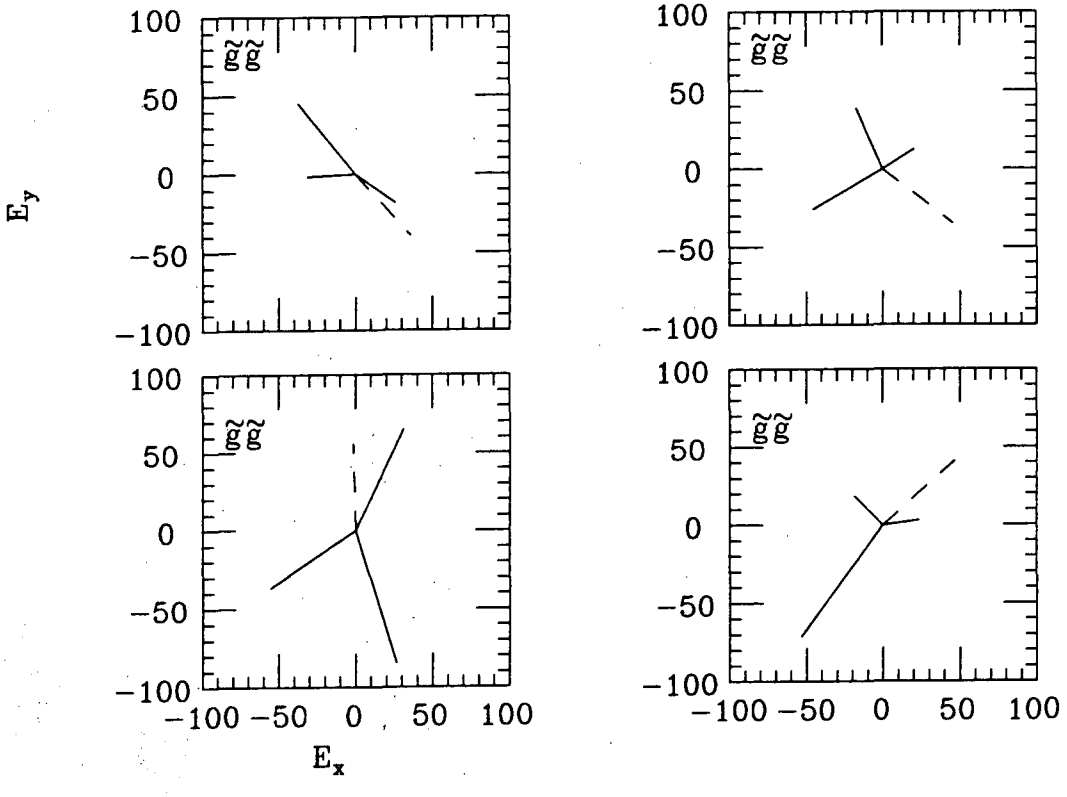

Figure 15. Simulated trijet events with large $E_T^{\rm miss}$ (shown with dashed line) from $\tilde{g}\tilde{g}$. The beam is perpendicular to the figure. The x and y axes are the energy of the jets in the x and y directions.

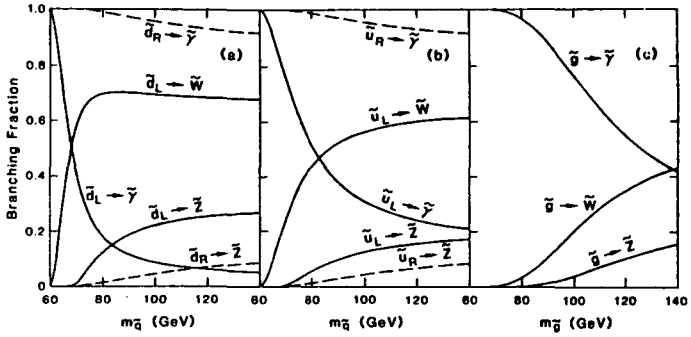

Figure 16. Branching fractions of $\tilde{q}$ and $\tilde{g}$ to $\tilde{\gamma}$, $\widetilde{W}$, and $\widetilde{Z}$ for masses accessible at Tevatron energies. Baer and Berger have taken $M_{\tilde{\gamma}} = 8$ GeV, $M_{\widetilde{W}} = 60$ GeV, and $M_{\widetilde{Z}} = 68$ GeV.

We plot our results in Figs. 17 and 18 as a function of the parameter μ for various choices of M and $\tan\beta(= v_2/v_1)$. For $M_{\tilde{q}} > 500$ GeV we find little difference from the results shown; for $M_{\tilde{q}} < 500$ GeV we find that the average branching ratio product generally increases. As shown, the greatest variation occurs with the parameter μ. Some differences in the curves occur because as μ increases, a different state becomes the LSP, and decay fractions to that state are different. When the curves are not shown at small μ, it is because for these parameters, the mass of the lightest chargino is $M(\tilde{\chi}^+) < 45$ GeV. Such light charginos can be discovered by lower energy machines long before SSC.

One can see that for most parameters of interest in the SSC region, the average product of branching fractions (which measures the suppression of the dijet plus very large missing energy signal) is not small. The suppression is generally a factor of $\frac{1}{10}$ to $\frac{1}{2}$ which represents no problem since the cross section

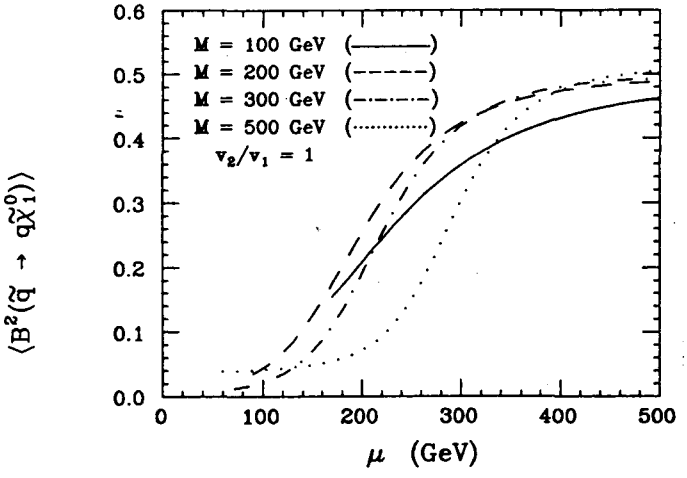

Figure 17. The average product of branching ratios for the $\tilde{q}$ pair to the LSP ($\tilde{\chi}_1^0$):

$$0.25[B^2(\tilde{u}_L) + B^2(\tilde{u}_R) + B^2(\tilde{d}_L) + B^2(\tilde{d}_R)].$$

The parameters as well as the rationale for ignoring $B(\tilde{u}_L)B(\tilde{u}_R)$, $B(\tilde{u}_R)B(\tilde{d}_R)$, etc. are discussed in the text.

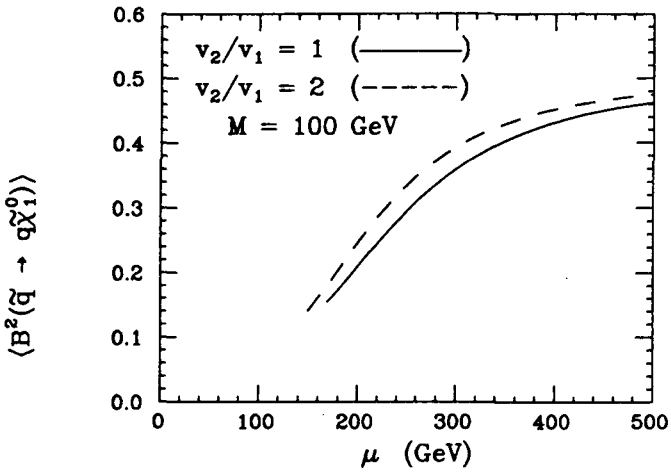

Figure 18. Same as for Fig. 17, but here we vary v_2/v_1.

is so large.

Of course, this implies that at least half the time there are other signals because at least one of the scalar quarks has decayed to a chargino $\tilde{\chi}^+$ or to a heavier neutralino, $\tilde{\chi}_2^0$ or $\tilde{\chi}_3^0$. The decays of these gauginos may or may not lead to interesting signals.

One question of interest in other sections of this report, is the probability of a scalar quark decaying to a heavier neutralino which in turn decays into $\tilde{\chi}_1^0$ and a photon:

$$\tilde{q} \to q\tilde{\chi}_2^0 \tag{3.41}$$

$$\tilde{\chi}_2^0 \to \gamma\tilde{\chi}_1^0 \tag{3.42}$$

This two-body decay occurs via a loop diagram. The competing decays are three-body decays occurring via tree-level processes:

$$\tilde{\chi}_2^0 \to \tilde{\chi}_1^0 f\bar{f} \quad \text{or} \quad \tilde{\chi}_1^+ f\bar{f} \tag{3.43}$$

In the SSC context where we assume $M_{\tilde{q}} \sim 500$ GeV ($v_2/v_1 \sim O(1)$, and M, $\mu \gtrsim 100$ GeV), contributions involving virtual scalar quarks are small compared with those involving virtual W and Z bosons. In this parameter range $\tilde{\chi}_1^0$ tends to have a substantial $\tilde{Z}^0$ component. $\tilde{\chi}_2^0$ and $\tilde{\chi}_3^0$ tend to have comparable masses and to be heavier than the lightest chargino, $\tilde{\chi}^+$; one is mostly $\widetilde{H}^0$ and the other is mostly $\tilde{\gamma}$. There is no reason to expect significant suppression of the 3-body modes, so the branching fraction for (3.42) tends to be of order 1–10%.

Given that the branching ratio for (3.41) could be as large as 50%, we see that even with a branching fraction for (3.42) of 1%, there should remain an important signal in $\tilde{q}\tilde{q}$ pair production of:

$$\tilde{q}_1 \to q\tilde{\chi}_1^0$$
$$\tilde{q}_2 \to q\tilde{\chi}_2^0 \qquad \tilde{\chi}_2^0 \to \gamma\tilde{\chi}_1^0$$

This leads to two energetic jets, large missing energy plus a very hard photon. Investigation of this signal will help us unravel the details of the supersymmetric model.

IV. Isolated Photons as Signals for Supersymmetry

In most early analyses of data, it has been assumed that the photino is the lightest supersymmetric particle (LSP). As discussed in the previous section, this is not in general true. One possibility is that the Higgsino, $\widetilde{H}^0$, is the LSP. However, because of its small coupling, its production in pp collisions is suppressed and it is rarely a direct decay product. As a consequence, one usually finds that it is the photino (or neutralino) that is initially produced, which then subsequently decays to the Higgsino:

$$\tilde{\gamma} \quad (\text{or} \quad \tilde{\chi}_i^0) \rightarrow \gamma \widetilde{H}^0 \tag{4.1}$$

We see that the observation of a hard photon along with missing energy can indicate the presence of supersymmetric processes. There are other scenarios in which one expects to find hard photons. One of these is discussed in the next section and in greater detail in a contribution to these proceedings by Barnett, Grifols, Gunion, Kalinowski, and Mendez.

Mikamo and Yamashita[13] in a contribution to these proceedings have examined the possibility of discovering supersymmetry via observation of a hard photon in the process

$$pp \rightarrow \tilde{g}\tilde{\gamma} \tag{4.2}$$

with

$$\tilde{\gamma} \rightarrow \gamma \widetilde{H}^0 \quad \text{and} \quad \tilde{g} \rightarrow q\bar{q}\tilde{\gamma} \tag{4.3}$$

In these events the Higgsinos carry off missing energy. Assumptions here are that branching fractions (4.3) are 100%, that $M_{\tilde{q}} > M_{\tilde{g}}$, $M_{\tilde{g}}$ = 100–200 GeV, $M_{\tilde{\gamma}}$ = 10–30 GeV, and $M_{\widetilde{H}^0}$ = 1–5 GeV.

Mikamo and Yamashita have considered three types of standard model backgrounds. The first are those from

$$pp \rightarrow \pi^0 \text{ (or } \eta^0) + \text{jets} \tag{4.4}$$

where the π^0 (or η^0) decays into photons which cannot be resolved for $E(\pi^0) \gtrsim 50$ GeV (giving the appearance of a single photon). They have calculated both events with light quark and gluon jets and events with heavy quark jets. The former depend on mismeasurement to generate fake E_T^{miss} whereas the latter have real E_T^{miss} from neutrinos.

A second background is direct photon production

$$pp \rightarrow \gamma + \text{jets} \tag{4.5}$$

These photons have a comparable yield as π^0, but should be better isolated from jets.

The final background is from

$$pp \rightarrow W + \gamma \qquad (W \rightarrow \ell\nu) \tag{4.6}$$

$$pp \rightarrow Z + \gamma \qquad (Z \rightarrow \nu\bar{\nu}) \tag{4.7}$$

where the W and Z decays provide the missing energy.

All of the above were calculated using ISAJET except (4.7) which was calculated by H. Baer. If no significant cuts are made, the sum of the Standard Model backgrounds completely dominates the supersymmetry signal. Mikamo and Yamashita discuss several possible cuts. The angle between the leading photon and $\vec{p}_T^{\text{miss}}$ was found to be not useful in separating signal and background. Similarly the total E_T within $R_\gamma = [(\Delta\eta)^2 + (\Delta\phi)^2]^{\frac{1}{2}} < 1$ of the photon was not useful. However requiring E_T with $R_\gamma < 0.2$ of the photon to be less than 20 GeV was effective. Also effective was a cut on the total E_T in the event to be less than 2500 GeV. With these cuts, their results suggest that the supersymmetric signal (from $\tilde{g}\tilde{\gamma}$) might dominate for E_T^γ or $E_T^{\text{miss}} > 0.5$ TeV.

R. Wagner took a different approach. The question he asked was what probability is there for observing a leading, isolated neutral particle in a jet (with particular concern for finding photons). This question is also of interest in general since it constitutes a significant background in a variety of "new" physics processes and since it contributes to triggering on isolated clusters in an electromagnetic calorimeter. The probability of a jet faking a high p_T photon was estimated by R. Wagner who studied the composition of QCD produced jets using the PHYTHIA Monte Carlo Event Generator and the JETSET jet fragmentation routine of Bengtsson and Sjostrand.[14] Two-jet events were generated from QCD interactions of initial-state quarks, anti-quarks, and gluons from proton-proton collisions at a center-of-momentum energy of 40 TeV. Two different runs of 3000 events each were made with minimum q_T of the hard scattering set to be greater than 30 or 50 GeV/c.

The probability estimated for faking a photon is obviously dependent on ones definition of an isolated gamma and the energy and spatial resolution of the electromagnetic calorimeter used to detect it. For this study Wagner defined a fake gamma event as a jet in which the leading particle has p_T greater than some minimum value and with no other particles having p_T greater than some cutoff. He has not made an isolation requirement on the cells surrounding the leading particle. Rather he has taken isolation to mean that the other particles in the jet are of low enough p_T as to be lost in the underlying "event" which is expected to include both contributions of a minimum bias type from the event giving the jet and contributions from multiple proton-proton collisions occurring within the bunch crossing. No calorimeter simulation has been done. He has merely uniformly segmented rapidity-phi space, constructed jets with a simple clustering algorithm, and studied the composition of the jets.

Jets were reconstructed using the JETSET supplied routine, LUCELL. This routine is a simple cluster algorithm that segments a selected pseudorapidty range into η-ϕ bins of equal size, searches for jet initiator bins over a given p_T threshold, and adds the p_T for all bins within a fixed η-ϕ distance of the initiator. For our study we used a pseudorapidity range of -5.5 to 5.5, and η-ϕ segmentation of 0.06 by 0.06, and a fixed jet radius of 1.0 in η-ϕ. The p_T threshold for the jet initiator was set to 5 GeV/c and a jet was required to have a minimum summed p_T of 20 GeV/c. LUCELL returned the number of jets found satisfying these criteria along with their location in η-ϕ and their summed p_T. Figures 19 and 20 are histograms of the number of jets with $p_T > 20$ GeV/c found per event by LUCELL and of the p_T spectrum of the jets.

For each event, each final-state particle was examined to determine which, if any jet it belonged to. During this process the particle type and p_T were recorded for the highest p_T and second highest p_T particle in each jet. These data were used to check for the occurrence of an isolated neutral particle in the jet.

In Table I we give the breakdown of leading particle type. There is very little dependence of leading particle type composition on q_T of the hard scattering. About 17% of the events had a leading π^0, which is the main source of fake gammas. Including etas and real gammas from jets brings the percentage of jets with a leading neutral particle giving mostly e-m energy to 24%. An examination of the jets indicates that, as is expected, the jet fragmentation properties do not depend on average on the leading particle type. Therefore, to get higher statistics we use all jets in our analysis and scale down any probabilities by the appropriate π^0 or neutral fraction.

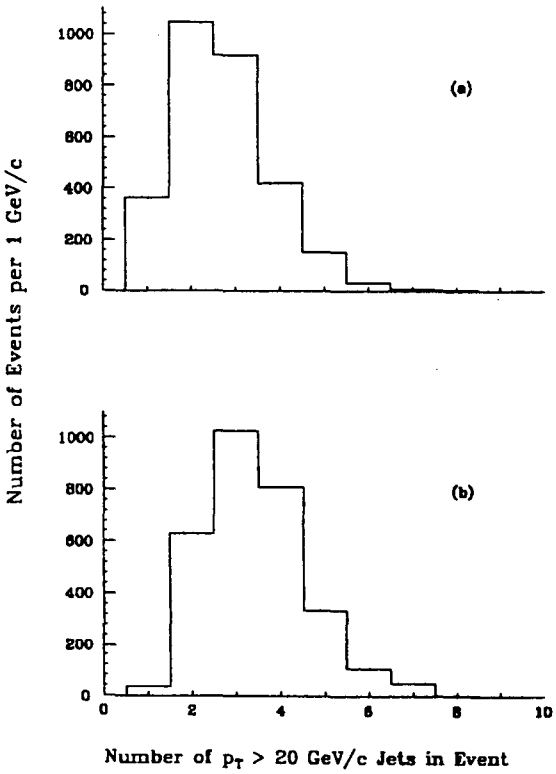

Figure 19. Number of jets found per event by LUCELL with $p_T > 20$ GeV/c using a jet initiator cell threshold of 5 GeV/c. (a) q_T minimum of hard scattering > 30 GeV/c. (b) q_T minimum of hard scattering > 50 GeV/c.

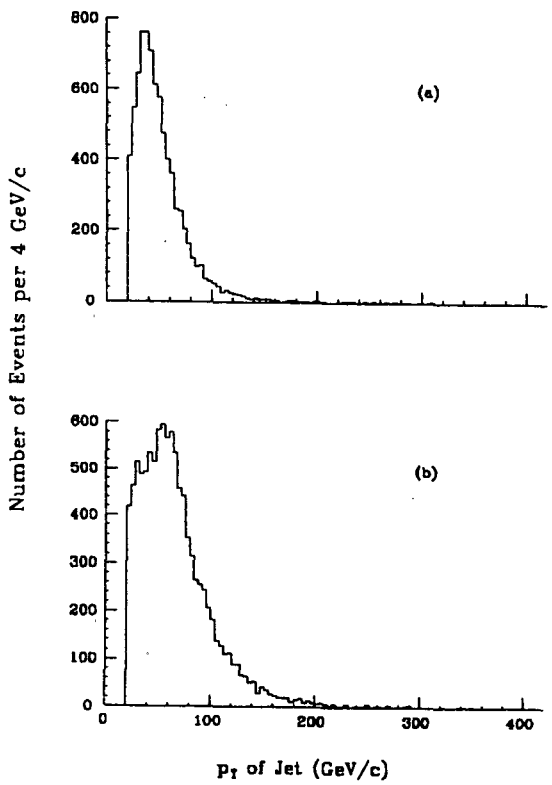

Figure 20. p_T spectrum of jets found by LUCELL. (a) q_T minimum of hard scattering > 30 GeV/c. (b) q_T minimum of hard scattering > 50 GeV/c.

Leading Particle Type	Jet p_T > 20 GeV/c	Jet p_T > 50 GeV/c
γ	0.43%	0.36%
$e^+ + e^-$	0.28	0.23
ν_e	0.27	0.26
$\mu^+ + \mu^-$	0.36	0.27
ν_μ	0.25	0.29
ν_τ	0.13	0.15
$\pi^+ + \pi^-$	35.19	35.95
$K^+ + K^-$	10.32	10.25
π^0	16.89	16.55
η	7.58	7.47
K_L^0	5.26	5.22
p	11.72	11.72
n	11.32	7.43

Table I. The Fraction of Total Jets with Given Leading Particle Type. These numbers are for $q_T^{\min} > 50$ GeV/c.

Figure 21 shows the probability of having a leading π^0 jet versus the second leading particle p_T for three different π^0 p_T cuts. The data shown are from the run with q_T minimum set to 50 GeV/c. Data from the 30 GeV/c run give the same results to within 25%. Errors on the curves range from about 15% for a second leading particle p_T cut of 10 GeV/c to 100% for a 2 GeV/c cut. The errors are also highly correlated since the plot is of a cumulative form. The probability to fake an isolated gamma drops quickly with increasing p_T of the π^0, but this trend stops above about 50 GeV/c. For π^0 minimum p_T cuts of 50–80 GeV/c, the probability of getting a leading π^0 with a given second leading particle p_T cut is constant to 25%; although the errors are quite large for p_T cuts above 50 GeV/c because of the small sample size. There are too few events

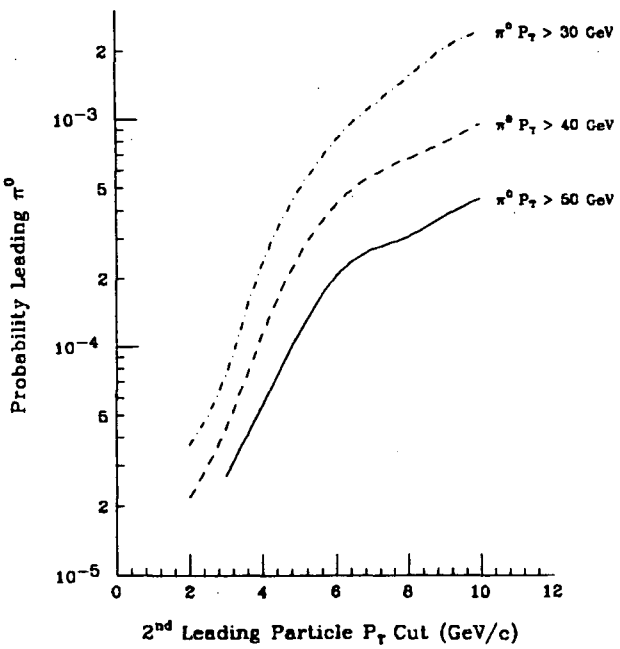

Figure 21. Probability of a leading π^0 with p_T greater than given cut versus p_T maximum cut for the second leading particle. Data shown are from run with q_T minimum of the hard scattering set to 50 GeV/c.

in the sample to make any estimates above a π^0 p_T-cut of 80 GeV/c. We conclude from this figure that it is straightforward to reduce the probability of getting a fake high p_T direct gamma from QCD jets to a level of a few $\times 10^{-5}$.

The above analysis is fairly naive and a number of complexities have been ignored. The events have not been put through a detector simulation to determine what effect calorimeter resolution or a magnetic field has on the results. Also we have concerned ourselves only with a leading neutral particle and have neglected contributions from events with a leading neutral cluster containing more than one particle. Finally one might be able to improve the rejection of fake gammas from this source with a more intelligent clustering algorithm. The expectations are, though, that these complications don't drastically change the results and one can trust the probability estimates to within a factor of two or three. Thus, one would expect that fake gammas can readily be eliminated with simple criteria to a level of 10^{-4} or better.

Morita[15] made an independent study of the probability of a QCD jet appearing to be a photon due to the presence of a leading π^0 (η^0) with little hadronic activity in a cone around it. He used ISAJET adapted to the CDF package, with a simple detector simulation. He studied the question of the criterion for the isolation cut of the electromagnetic cluster and also looked at the fragmentation properties of jets and the energy spectrum of the next-to-leading particle among jet fragments. Morita concluded that the probability of a QCD jet behaving like a single electromagnetic cluster is about 2–5$\times 10^{-4}$ for $E_T^{\rm jet} \geq 100$ GeV, and argues that tracking information will probably allow an even greater suppression.

V. Detection of a Higgs Boson via Its Supersymmetric Decay

In all supersymmetric models there are at least two Higgs doublets. One of the two neutral Higgs scalars (H_2^0) may be light and resembles the Standard Model Higgs. By contrast the heavier neutral scalar (H_1^0) is expected to have very different couplings.[16] In particular if $m(H_1^0) \gtrsim 200$ GeV, then its couplings to W and Z pairs are greatly suppressed, and it is possible (depending on masses) that decays to charginos and neutralinos are very important. This is discussed in detail in a contribution to these proceedings by Barnett, Grifols, Gunion, Kalinowski, and Mendez[17] (BGGKM).

The process considered involves the production of the heavy Higgs, H_1^0 via the t quark content of the proton or via gluon-gluon fusion:

$$gg \quad \text{or} \quad t\bar{t} \to H_1^0 \to \widetilde{H}^0 \tilde{Z}^0 \tag{5.1}$$

with

$$\widetilde{H}^0 \to \gamma\tilde{\gamma} \tag{5.2}$$

$$\tilde{Z}^0 \to \ell^+\ell^-\tilde{\gamma} \tag{5.3}$$

In order to show a representative case, BGGKM take

$$\begin{aligned} &M(H_1^0) = 400 \text{ GeV} \qquad M(\widetilde{H}^0) = 10 \text{ GeV} \\ &M(\tilde{Z}^0) \approx m(Z) \qquad M(\tilde{q}), M(\tilde{\ell}) > 100 \text{ GeV} \end{aligned} \tag{5.4}$$

In this case, we find from Ref. 16

$$B(H_1^0 \to \widetilde{H}^0 \tilde{Z}^0) = 0.25 \tag{5.5}$$

The resulting final state is

$$\ell^+\ell^-\gamma + \text{ missing energy.} \tag{5.6}$$

Whether or not this particular scenario turns out to be realistic, it is worthwhile (as a general new physics search technique) considering the detectability of final states involving hard photons but no high-energy jets.

The total integrated cross section for process (5.1) is 0.26 pb. In order to reduce the backgrounds discussed below, BGGKM impose a variety of cuts. These are:

$$\begin{aligned} &E_\gamma > 50 \text{ GeV} \qquad 30 < M(\ell^+\ell^-) < 83 \text{ GeV} \\ &M(\ell^+\ell^-\gamma) > 200 \text{ GeV} \qquad E_T^{\rm miss} > 50 \text{ GeV} \\ &\theta(\vec{p}_T^{\,\gamma}, \vec{p}_T^{\,\rm miss}) < 60^\circ \quad \text{or} \quad > 120^\circ \\ &|\theta(\ell^\pm, \gamma)| > 10^\circ \quad \text{and} \quad |\theta(\gamma, \text{beam})| > 10^\circ \end{aligned} \tag{5.7}$$

The signal cross section is reduced to 0.04 pb by these cuts. This corresponds to 400 events/year assuming an integrated luminosity of 10^{40} cm^{-2} (or of 10^4 pb^{-1}) per year.

The backgrounds for this process include

$$a) \quad t\bar{t} \to \widetilde{H}^0\tilde{Z}^0 \quad \text{(non-resonant)} \tag{5.8}$$

$$b) \quad q\bar{q} \to \ell^+\ell^-\gamma \quad \text{(via } Z^* \text{ and } \gamma^*\text{)} \tag{5.9}$$

$$c) \quad q\bar{q} \to \pi^0 Z^* \quad (Z^* \to \ell^+\ell^-) \tag{5.10}$$

$$d) \quad q\bar{q} \to W^+W^- \quad (W^\pm \to \ell^\pm\nu) \tag{5.11}$$

$$e) \quad q\bar{q} \to Z^*Z\gamma \quad (Z^* \to \ell^+\ell^-; Z \to \nu\bar{\nu}) \tag{5.12}$$

BGGKM calculated *a*) and *b*) in detail. The continuum process *a*) was found to be very small, whereas *b*) is the only substantial background. The others (*c*-*e*) were estimated to be small. Without fine-tuning the the cuts, process *b*) can be reduced to a fourth of the signal. Furthermore if we define an effective Higgs mass (approximating the mass of H_1^0) as

$$M_{\rm eff}^2 = M^2(\ell^+\ell^-\gamma) + 2E_T^{\rm miss}E^{\rm obs} - 2\vec{p}_T^{\,\rm miss} \cdot \vec{p}_T^{\,\rm obs} \tag{5.13}$$

then we find that the $M_{\rm eff}$ distribution, Fig. 22 shows a significant peak for the signal but not for the background.

We conclude, therefore, that judicious choices of cuts can be used to clearly separate a small but distinctive signal from background. In this case it is the heavier Higgs boson of super-

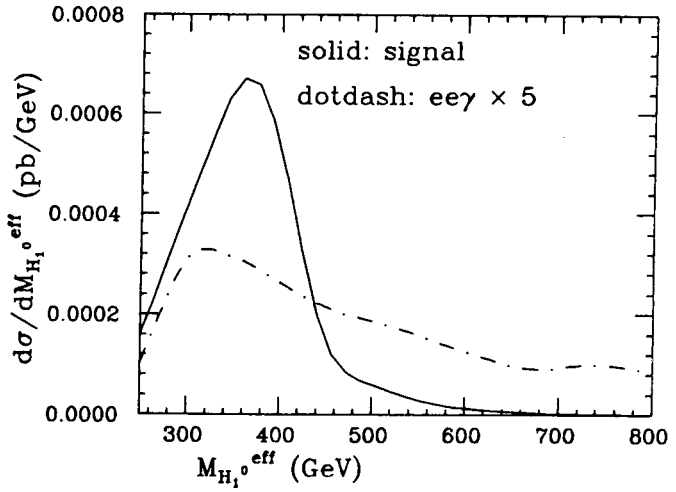

Figure 22. The distribution of $M_{\rm eff}(H_1^0)$ as defined by Eq. 5.13 for the $H_1^0 \to \widetilde{H}^0\tilde{Z}^0$ signal (solid) and for the dominant background (dashes) given by Eq. 5.9. All of the cuts described in the text were imposed except for those involving missing momentum or energy. Fake missing momentum was generated randomly for the background according to a plausible distribution.

symmetry which would be discovered via its supersymmetric decay modes.

VI. Detection of Charginos and Neutralinos

During the last two years, there has been considerable attention to the production of winos and zinos at the Sp$\bar{p}$S and Tevatron colliders.[18] These papers have considered

$$\bar{p}p \to \widetilde{W}\tilde{\gamma} + X \tag{6.1}$$
$$\bar{p}p \to \widetilde{W}\tilde{Z} + X \tag{6.2}$$
$$\bar{p}p \to \widetilde{W}\widetilde{W} + X \tag{6.3}$$
$$\bar{p}p \to \tilde{Z}\tilde{\gamma} + X \tag{6.4}$$
$$\bar{p}p \to \tilde{Z}\tilde{Z} + X \tag{6.5}$$

These may occur via W or Z boson decay if kinematically allowed (e.g. — $W \to \widetilde{W}\tilde{\gamma}$). There are other processes such as $\widetilde{W}\tilde{q}$ or $\widetilde{W}\tilde{g}$ production which have received less attention since their signals are not as distinctive.

Once produced the decays include:

$$\widetilde{W} \to q\bar{q}'\tilde{\gamma} \quad \text{or} \quad \ell\bar{\nu}\tilde{\gamma} \tag{6.6}$$
$$\tilde{Z} \to q\bar{q}\tilde{\gamma} \quad \text{or} \quad \ell\bar{\ell}\tilde{\gamma} \tag{6.7}$$
$$\tilde{Z} \to q\bar{q}'\widetilde{W} \quad \text{or} \quad \ell\bar{\nu}\widetilde{W} \tag{6.8}$$

Baer, Hagiwara, and Tata[19] observe that this latter decay would become important when $M_{\tilde{q}}, M_{\tilde{\ell}} > 350$ GeV for $M_{\tilde{Z}} = 45$ GeV. If $M_{\tilde{q},\tilde{\ell}} > M_{\widetilde{W},\tilde{Z}}$, then these decays are 3-body decays. If $M_{\tilde{q}}, M_{\tilde{\ell}} < M_{\widetilde{W},\tilde{Z}}$, then 2-body decays to scalar quarks and leptons would dominate. Finally, if $M_{\widetilde{W}} > M_W$, we must consider

$$\widetilde{W} \to W\tilde{\gamma}. \tag{6.9}$$

The processes (6.2) and (6.3) lead with some branching fraction to multi-leptons plus large $E_T^{\rm miss}$. These are discussed elsewhere in the context of the Tevatron collider.

The processes producing $\widetilde{W}\tilde{\gamma}$ can give a single lepton plus very large missing energy. At first glance this seems to be an excellent signal. But as can be seen in Fig. 23, at Tevatron energies this signal ($W \to \widetilde{W}\tilde{\gamma}$) is buried in the background ($W \to e\nu$ or $\tau\nu$) without being distinctive.

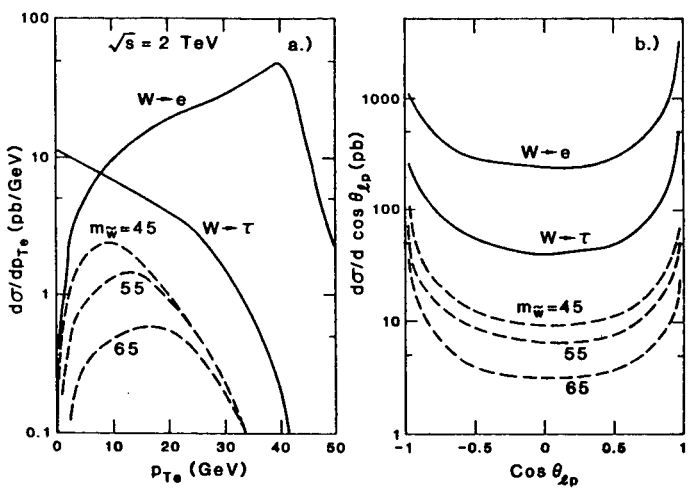

Figure 23. Distributions for the process $pp \to W + X$ where $W \to \widetilde{W} + \tilde{\gamma}$, $\widetilde{W} \to e\nu\tilde{\gamma}$ (dashed) or $W \to e\nu, \tau\nu$ (solid). These curves for the Tevatron collider were made by Baer and Tata.

This signal has been analyzed by Ukegawa, Takaiwa, and Kondo (UTK) at this workshop for SSC energies. They take $M_{\widetilde{W}} = 250$–500 GeV and make the simplifying assumptions that the photino is very light and a pure state. The backgrounds they consider are

$$pp \to W + X \qquad (W \to \ell\nu) \tag{6.10}$$
$$pp \to W + Z + X \qquad (W \to \ell\nu \text{ and } Z \to \nu\bar{\nu}) \tag{6.11}$$

Using ISAJET, UTK find the following cross sections before cuts:

$(W \to e\nu)$	4.5×10^4 pb
$(W \to e\nu) + (Z \to \nu\bar{\nu})$	0.89 pb
$(\widetilde{W} \to W \to e\nu) + \tilde{\gamma}$	0.22 pb $M_{\widetilde{W}} = 250$ GeV
	0.05 pb $M_{\widetilde{W}} = 500$ GeV

They then examine the E_T^e and $E_T^{\rm miss}$ distributions. To the extent that the W is produced at rest in the transverse plane, the W background could be eliminated by requiring $E_T^e > 100$ GeV and/or $E_T^{\rm miss} > 100$ GeV. The $W + Z$ background drops below the signal when these cuts are made at 200 GeV (with these cuts the signal has been reduced severely). UTK next study the transverse mass of the electron and missing energy:

$$M_T^2 \equiv 2p_T^e p_T^{\rm miss}(1 - \cos\phi) \tag{6.12}$$

Making cuts in M_T and assuming an integrated luminosity of 10^{40} cm^{-2}, UTK find that the background due to real W's is entirely removed, and the signal and $W + Z$ background are:

for $M_T > 300$ GeV

11 events	for $M_{\widetilde{W}} = 250$ GeV
63 events	for $M_{\widetilde{W}} = 500$ GeV
52 events	background

for $M_T > 400$ GeV

1.1 events	for $M_{\widetilde{W}} = 250$ GeV
28 events	for $M_{\widetilde{W}} = 500$ GeV
0.4 events	background

Clearly this process ($\widetilde{W} + \tilde{\gamma}$) will not be useful at SSC energies unless $M_{\widetilde{W}} > 250$ GeV. It suggests that more attention should be given to the $\widetilde{W} + \tilde{Z}$ and $\widetilde{W} + \widetilde{W}$ processes which yield more distinctive signals.

VII. Conclusions

The supersymmetry working group at Snowmass has examined in detail several missing energy signals. We have taken advantage of theoretical and experimental progress which has taken place in the two years since the last Snowmass Summer Study.

In addition to the theoretical advances described in this report, a project developing the proper methods for calculating the distributions of heavy particles in the proton was completed in Snowmass (and is described in Ref. 20). That work is relevant to supersymmetry since it can describe initial-state gluino-quark scattering. The distribution of t quarks is important to the work of Sec. V (describing $H^0 \to \tilde{Z}^0\widetilde{H}^0$).

Our knowledge of the appropriate techniques for searching for supersymmetry was greatly refined by examination of results from the Sp$\bar{p}$S hadron collider. More can be learned from experiments which will soon begin at the Tevatron collider. Our studies indicate, however, that a comprehensive understanding of the structure of the supersymmetric theory cannot be obtained without the availability of a collider with the power of the SSC.

References

1. H.E. Haber and G.L. Kane, Phys. Reports **117**, 75 (1985); J. Ellis, in *Proceedings of the 1985 International Conference on Lepton and Photon Interactions at High Energies, August 19–24, 1985, Kyoto*, edited by M. Konuma and K. Takahashi (Kyoto University, Kyoto, Japan 1986) p. 242; R.M. Barnett, in *Proceedings of the 19th SLAC Summer Institute on Particle Physics — Supersymmetry, July 1985*, edited by E.C. Brennan (SLAC, Stanford, California, 1986) p. 95 (also report no. LBL-20492).
2. H. Baer, D. Karatas, and X. Tata, Wisconsin report no. MAD/PH/310 (1986).
3. M. Davier, rapporteur talk at the XXIII International Conference on High Energy Physics, Berkeley, 16–23 July 1986.
4. H-U. Bengtsson and T. Sjostrand, Pythia Version 4.7 July 1986; T. Sjostrand, Jetset Version 6.2 June 1986, LU-TP-85-10, October 1985.
5. F. Paige and S. Protopopescu, ISAJET Version 5.20. For writeup see F. Paige and S. Protopopescu, BNL-37271, August 1985.
6. R.M. Barnett, H.E. Haber, and G.L. Kane, Nucl. Phys. **B267**, 625 (1986); see also M.J. Herrero et al., Phys. Lett. **132B**, 199 (1983); J. Ellis and H. Kowalski, Nucl. Phys. **B246**, 189 (1984) and Nucl. Phys. **B259**, 109 (1985); E. Reya and D.P. Roy, Phys. Lett. **166B**, 223 (1986) and Dortmund report no. DO-TH-86/06 (1986); V. Barger et al., Phys. Rev. **D33**, 57 (1986); A.De Rujula and R. Petronzio, Nucl. Phys. **B261**, 587 (1985); and Ref. 10.
7. G. Arnison et al., report no. CERN-EP/82-122 (1982).
8. G. Arnison et al., Phys. Lett. **132B**, 214 (1983); P. Darriulat, in *Proceedings of the 19th SLAC Summer Institute on Particle Physics — Supersymmetry, July 1985*, edited by E.C. Brennan (SLAC, Stanford, California, 1986) p. 163 (also CERN-EP/85-167).
9. S. Dawson et al., *Proceedings of the 1984 summer Study on the Design and Utilization of the Superconducting Super Collider, Snowmass, Colorado*, edited by R. Donaldson and J. Morfin, (Fermilab, Batavia, Illinois, 1984) p. 263.
10. C. Rubbia, in *Proceedings of the 1985 International Conference on Lepton and Photon Interactions at High Energies, August 19–24, 1985, Kyoto*, edited by M. Konuma and K. Takahashi (Kyoto University, Kyoto, Japan 1986) p. 242; A. Honma, invited talk at the XXIII International Conference on High Energy Physics, Berkeley, 16–23 July 1986, report no. CERN-EP/86-153.
11. H. Baer and E.L. Berger, Phys. Rev. **D34**, 1361 (1986).
12. R.M. Barnett and H.E. Haber, report in preparation.
13. S. Mikamo and A. Yamashita, contribution to these proceedings.
14. H-U. Bengtsson and T. Sjostrand, Pythia Version 4.7 July 1986; T. Sjostrand, Jetset Version 6.2 June 1986, LU-TP-85-10, October 1985.
15. Y. Morita, contribution to these proceedings.
16. J.F. Gunion and H.E. Haber, U.C. Davis report no. UCD-86-12 (1986).
17. R.M. Barnett, J.A. Grifols, J.F. Gunion, J. Kalinowski, and A. Mendez, contribution to these proceedings, U.C. Davis report no. UCD-86-20 (1986).
18. H. Baer, K. Hagiwara, X. Tata, reports no. MAD/PH/296 (1986) and MAD/PH/298 (1986); R. Arnowitt and P. Nath, Northeastern reports nos. NUM-2699 (1986) and NUM-2704 (1986); P. Nath, R. Arnowitt, and A. Chamseddine, Phys. Lett. **129B**, 445 (1983) and **174B**, 399 (1986); D. Dicus, S. Nandi, and X. Tata, Phys. Lett. **129B**, 451 (1983); V. Barger et al., Phys. Lett. **131B**, 372 (1983); P. Fayet, Phys. Lett. **133B**, 363 (1983); D. Dicus et al., Phys. Rev. **D29**, 67 (1984); G. Altarelli et al., Nucl. Phys. **B245**, 215 (1984); R.M. Barnett and H.E. Haber, Phys. Rev. **D31**, 85 (1985); S. Gottlieb and T. Weiler, Phys. Rev. **D32**, 1119 (1985).
19. H. Baer, K. Hagiwara, X. Tata, report no. MAD/PH/296 (1986).
20. H.E. Haber, D.E. Soper, R.M. Barnett, U.C. Santa Cruz report no. SCIPP-86/70 (1986).

LAWRENCE BERKELEY LABORATORY
TECHNICAL INFORMATION DEPARTMENT
UNIVERSITY OF CALIFORNIA
BERKELEY, CALIFORNIA 94720